

# Beam halo experiment at IHEP\*

PENG Jun(彭军)<sup>1)</sup> HUANG Tao(黄涛) LIU Hua-Chang(刘华昌) JIANG Hong-Ping(蒋洪平)  
 LI Peng(李鹏) LI Fang(李芳) LI Jian(李健) LIU Mei-Fei(刘美飞) MU Zhen-Cheng(慕振成)  
 MENG Cai(孟才) MENG Ming(孟鸣) OUYANG Hua-Fu(欧阳华甫) RONG Lin-Yan(荣林艳)  
 TIAN Jian-Min(田建民) WANG Biao(王标) WANG Bo(王博) XU Tao-Guang(徐韬光)  
 XU Xin-An(徐新安) YAO Yuan(姚远) XIN Wen-Qu(辛文曲) ZHAO Fu-Xiang(赵富祥)  
 ZENG Lei(曾磊) ZHOU Wen-Zhong(周文中)

Accelerator Center, Institute of High Energy Physics, Chinese Academy of Sciences, Beijing 100049, China

**Abstract:** Space-charge forces acting in mismatched beams have been identified as a major cause of beam halo. In this paper, we describe the beam halo experimental results in a FODO beam line at IHEP. With this beam transport line, experiments are carried out to compare the measured data with the multi-particle simulations and to study the formation of a beam halo. The maximum measured amplitudes of the matched and mismatched beam profiles agree well with simulations. Details of the experiment are presented.

**Key words:** high intensity, proton, halo, multi-particle simulation

**PACS:** 29.20.Ej, 83.10.Pp, 87.15.A- **DOI:** 10.1088/1674-1137/37/3/037002

## 1 Introduction

Nowadays, high-power and high-intensity proton beams are widely required in applications such as neutron spallation sources, transmutation of nuclear waste, accelerator driven sub-critical systems (ADS), etc. The existence of halo is an important characteristic of high-intensity beams. Because halo particles in proton linacs tend to be lost on the walls of the beam line structures and induce unwanted radioactivity, the interest in understanding the halo formation has increased.

Space-charge forces acting in mismatched beams have been commonly identified as a major cause of beam halo. It is found that the mismatch can produce coherent oscillations of the RMS beam size. Individual beam particles interact with the time-varying space charge field due to the plasma oscillation in the beam core, acquire enough transverse energy and then become parts of the halo [1]. In order to understand this process, large numbers of theoretical literatures [2] have been produced and large numbers of computer simulations have been carried out [3]. However, few beam experiments have been done, owing in part to the fact that few intense proton beams with the required intensity exist [4]. Fortunately, by making use of the available intense proton beams from a radio frequency quadrupole (RFQ) accelerator designated

for ADS study at the Institute of High Energy Physics (IHEP), we have set up a 28-quadrupole beam transport line as the platform to study the beam halo experimentally. It is the first domestic beam line dedicated to the halo study of high intensity proton beams. By comparing the experimental data with the multi-particle simulations, halo characteristics can be better understood.

## 2 The beam halo experiment transport line

The 28-quadrupole beam transport line is installed after the IHEP RFQ with an output energy of 3.5 MeV and an operating frequency of 352 MHz. The purpose of this transport line is the experimental study of the beam halo formation and the comparison of the measured data and halo simulations. The layout of this transport line is shown in Fig. 1. In this line, the first four quadrupoles are used to establish matching or different mismatch conditions for the halo formation and the last 24 quadrupoles are used to form an FODO lattice. The quadrupoles are spaced every 19 cm so that beam diagnostic devices can be mounted between the magnets. Table 1 shows the beam pipe diameters, the quadrupole lengths and gradients. Since the predicted matched RMS beam radius is about 0.15 cm, the beam pipe diameter is designed to

Received 25 April 2012

\* Supported by NSFC (91126003) and the State Key Development Program of Basic Research of China (2007CB209904)

1) E-mail: pengjun@mail.ihep.ac.cn

©2013 Chinese Physical Society and the Institute of High Energy Physics of the Chinese Academy of Sciences and the Institute of Modern Physics of the Chinese Academy of Sciences and IOP Publishing Ltd

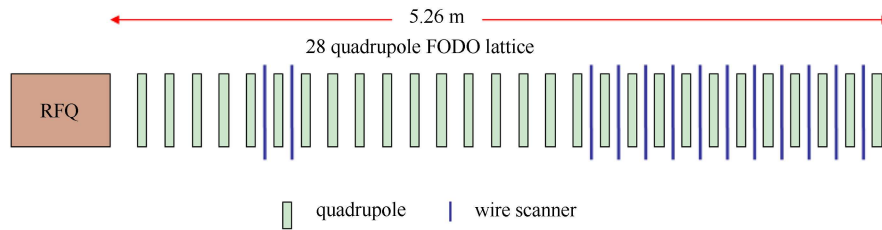


Fig. 1. Layout of the beam halo experiment transport line.

Table 1. Parameters of the beam halo experiment transport line.

quadrupole number	1	2	3	4	5-28
beam pipe diameter/cm	3.6	3.6	3.6	3.6	3.6
Max magnet gradient/(T/m)	30	30	30	30	30
magnet length/cm	10.5	10.5	10.5	10.5	7

be 3.6 cm, which is more than 10 times the RMS beam size.

In the transport line, an array of up to fourteen scanners is used to monitor the beam profiles over the whole transport line. Each scanner consists of a 32 micron diameter carbon filament for the measurement of the dense beam core and a pair of 1.5 mm thick scraper plates for the measurement of the low-density halo region [5]. The beam-profile scanner can provide intensity measurements over a dynamic range of about  $10^5$ . The philosophy for the scanner placement is the following: the first group of two scanners is placed after quadrupoles 5 and 6. They are used to measure the beam distribution at the exit of the RFQ and provide a critical initial condition on the halo evolution. The computer simulations show that the RMS mismatched beams evolve and form a long period envelope oscillation in the linear focusing beam transport line. Although the oscillation amplitude depends on the mismatch strength, the period is only related to the focusing strength and not the mismatch strength. With the zero current phase advance of  $66.9^\circ$  per period, about 4 mismatch oscillations will develop along the transport line. To observe halo formation, another two groups of scanners with 6 scanners for each group are placed after quadrupole 17 to 28, covering completely two full mismatch oscillations. The scanners of the first and the second group are used to monitor the beam profile in  $x$  direction and  $y$  direction alternately. The scanners of the third group are all used to monitor the beam profiles in  $x$  direction.

### 3 Comparison between simulation and experiment

The output beam from the IHEP RFQ is used in the experiments. The beam current is about 20 mA. To avoid beam destruction of the thin wires used for measurement of the beam profiles, the beam is pulsed

at a repetition rate of 1 Hz and a pulse length of 50-microsecond. Due to the lack of detailed knowledge of the initial beam distribution at the exit of RFQ in advance, three different initial distributions are generated in the simulations, i.e.: (1) 6D Gaussian, (2) a distribution called RFQ-1, generated from a simulation of the RFQ with the transmission rate of 98.1% [6], (3) a distribution called RFQ-2, generated from a simulation of the RFQ with the transmission rate of 70%. During the experimental process, since the RF power fed into RFQ is lower than the designed value due to an old klystron, the actual RFQ transmission rate is much smaller than the designed value. This is why two simulation distributions of the RFQ are used. The RFQ-2 distribution may be closer to the experimental beam than the other two distributions. The 6D Gaussian distribution has the same Courant-Snyder parameters as the RFQ-1 distribution. The transverse phase-space plots of these distributions are given in Fig. 2. As shown in Fig. 2, the halo in the two RFQ distributions is more obvious than that in the Gaussian distribution and the trace-space ellipse filament is observed in the RFQ-2 distribution. With these three initial distributions at an input beam current of 20 mA, simulations are carried out for the beam transportation through the 28-quadrupole beam transport line with the PARMILA code [7]. In general, 50000 macro-particles per bunch are used in simulations. The space-charge interaction is calculated via the 2-dimensional particle in cell (PIC) method with a  $40 \times 40$  mesh and the mesh size is 0.05 cm. In the simulations, the parameters of the 28 quadrupoles adopted are exactly the same as those in the experiments.

In the experiments, the first four quadrupoles were adjusted to produce matching. The matching quadrupole gradients are obtained by producing an equal rms beam size at different locations and the rms beam sizes are calculated from the measured beam profiles. The density profiles of the matched beam from simulations and from measurements are compared and shown in Figs. 3 and 4. As shown in the two figures, in the middle of the beam transport line, the simulated beam profiles are smaller than the measured ones. At the end of the beam transport line, the simulated profile from the RFQ-2 distribution agrees well with the measured one, and the simulated profiles from the other two distribu-

tions are slightly smaller than those from the measurement. The results show that, in the matched case, the profiles from the simulated distributions are in good agreement with the shape of the measured profiles. The result obtained above provides good guidance for the beam pipe design of a linac that runs at about 20 mA beam current.

The first four quadrupoles are also adjusted to produce mismatch. A comparison of the mismatched beam profiles between the simulated and the measured ones is shown in Figs. 5 and 6. As shown in the two figures, all three simulations predict the maximum beam size well, however, unlike the matched case, they fail to reform the

shape of the measured profile. For the simulated beams, the particle density differences between the core and the tail are in the order of  $10^3$ . The simulated beams tend to form a uniform core with a short extent edge rather than a halo. For the measured beam, the particle density differences between the core and the tail are in the order of  $10^4$ . The measured profile shows broader shoulders and asymmetric features, which are the prominent features of a halo in mismatched beams [8]. We also checked the beam profiles after each quadruple along the beam line for simulated mismatched beams and did not find these features. It illustrates that no halo forms in the simulated beams. After that, we investigated the effects

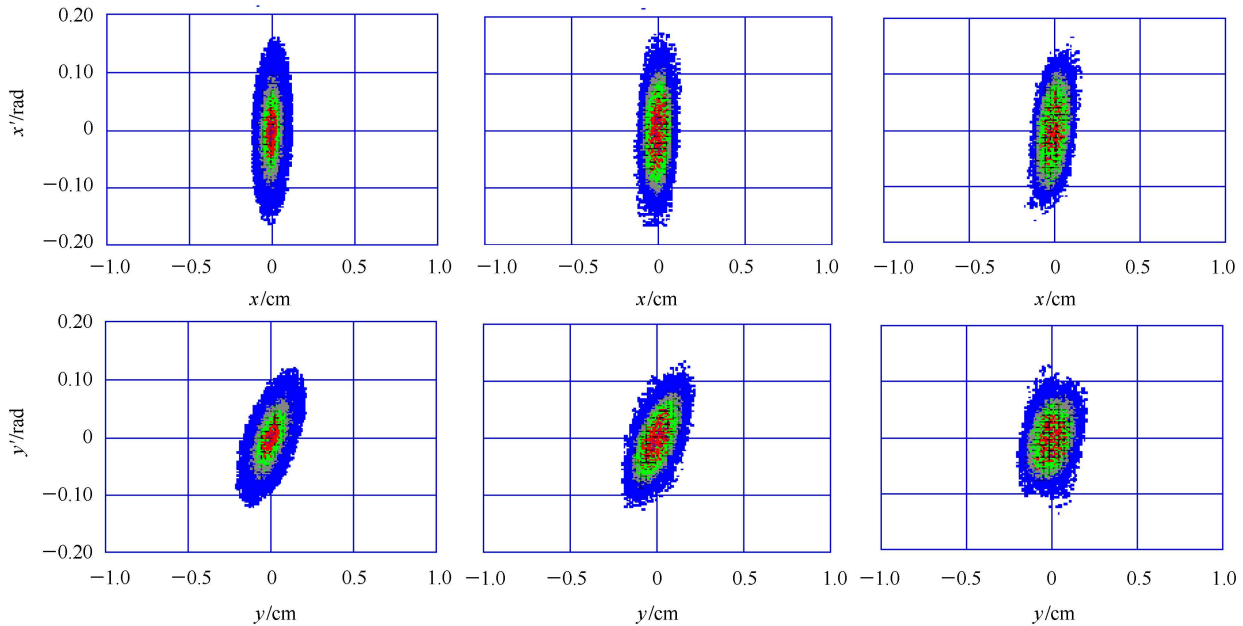


Fig. 2. The transverse phase-space projections for three initial simulation distributions: 6D Gaussian (left), RFQ-1 (middle) and RFQ-2 (right). The upper plots show the  $x-x'$  phase space, and the lower plots show the  $y-y'$  phase space.

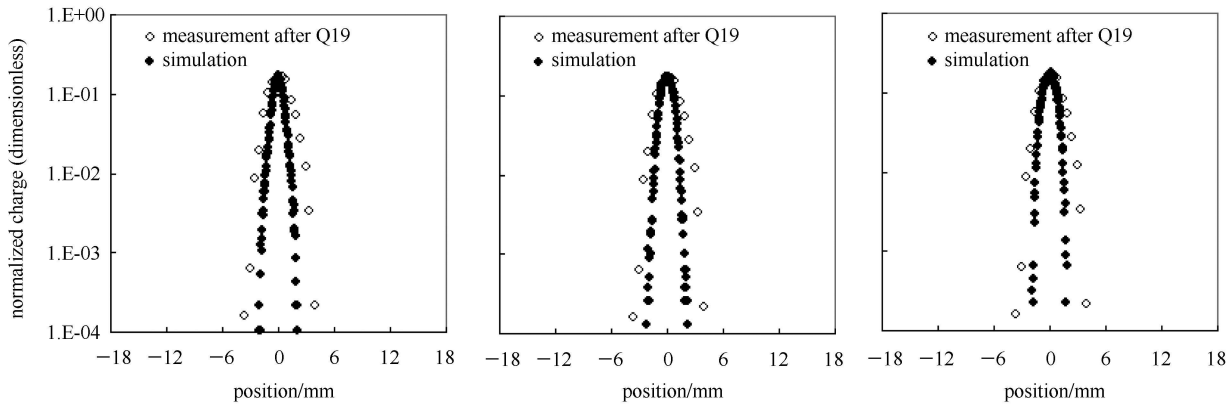


Fig. 3. The horizontal profiles from measurements (circles) and simulations (dots) at the 5<sup>#</sup> wire scanner for 20 mA matched beam. The initial distributions for the simulations are: 6D Gaussian (left), RFQ-1 (middle), and RFQ-2 (right).

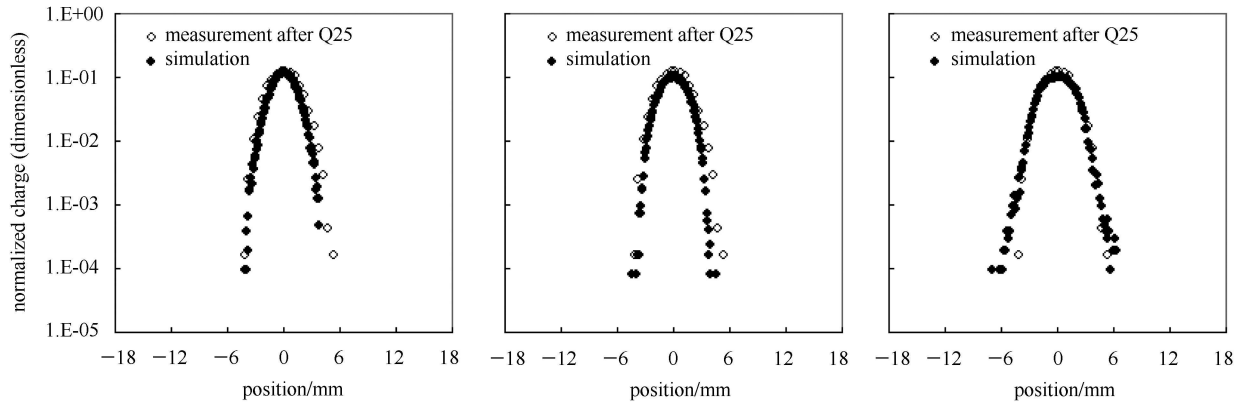


Fig. 4. The horizontal profiles from measurements (circles) and simulations (dots) at the 11<sup>#</sup> wire scanner for 20 mA matched beam. The initial distributions for the simulations are: 6D Gaussian (left), RFQ-1 (middle), and RFQ-2 (right).

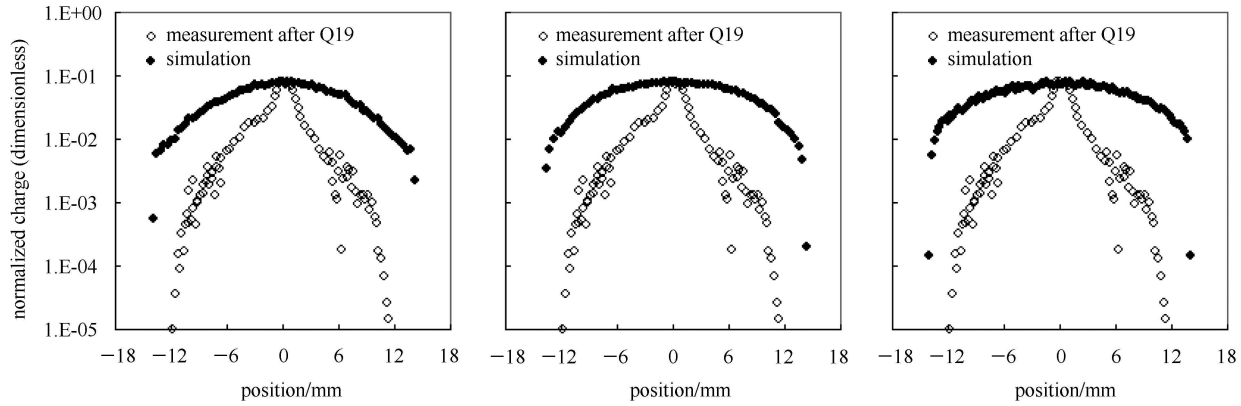


Fig. 5. The horizontal profiles from measurements (circles) and simulations (dots) at the 5<sup>#</sup> wire scanner for 20 mA mismatched beam. The initial distributions for the simulations are: 6D Gaussian (left), RFQ-1 (middle), and RFQ-2 (right).

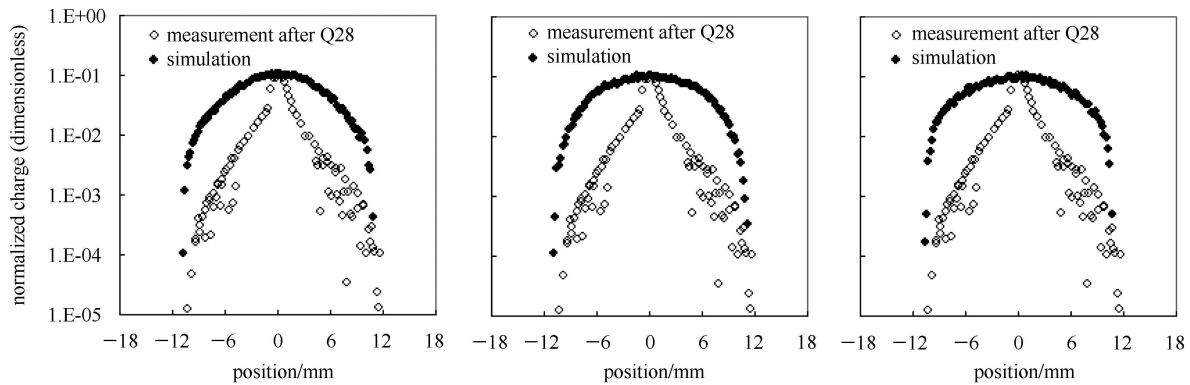


Fig. 6. The horizontal profiles from measurements (circles) and simulations (dots) at the 14<sup>#</sup> wire scanner for a 20 mA mismatched beam. The initial distributions for the simulations are: 6D Gaussian (left), RFQ-1 (middle), and RFQ-2 (right).

of mesh sizes and used a 3D PIC code to calculate the nonlinear space charge force. However, the results show no significant change. To approach the measured beam, we added the manufacturing errors of magnets in simulations and found that the simulated beam profiles with errors are nearly the same as those without errors except for a small quantity of beam center shift.

## 4 Conclusions

We have compared the multi-particle simulations of a 20 mA beam with the measurement data. Three different initial distributions were used: 6D Gaussian and two distributions determined from multi-particle simu-

lations through the RFQ. The maximum amplitudes of the measured beam are consistent with the predictions from numerical simulations. The simulated profiles of the matched beam are in good agreement with the measurement. However, the computer simulations failed to reproduce the shape of the measured mismatched profiles. The measured mismatched beam profiles exhibit prominent shoulders, which are not observed in the simulated beams. The effects of mesh sizes, calculation methods of space charge force and magnet errors are studied with no significant change in results. Since the maximum number of particles and the mesh number of 3D space charge calculation of the PARMILA code are constrained in a small range, we need to do more simulations using other multi-particle codes.

---

## References

- 1 Reiser M. Theory and Design of Charged Particle Beams. New York: John Wiley & Sons, 1994
- 2 Wangler T P, Crandall K R, Ryne R et al. Phys. Rev. ST Accel. Beams, 1998, **1**: 084201
- 3 QIANG J, Colestock P L, Gilpatrick D et al. Phys. Rev. ST Accel. Beams, 2002, **5**: 124201
- 4 Colestock P L, Wangler T, Allen C K. The Beam Halo Experiment at LEDA. Proc. of the XX International Linac Conference. Monterey, California, 2000. 806–808
- 5 RUAN Y F. The Study of the Beam Instruments for CSNS Linac (Ph.D. Thesis). Beijing: Institute of High Energy Physics, CAS, 2010(in Chinese)
- 6 GUAN X L, LUO Z H, FU S N. Chinese Journal of Nuclear Science and Engineering, 2003, **23**(1): 73–78
- 7 Harunori T. PARMILA. LA-UR-98-4478, 1998, Revised July 26, 2005
- 8 Wangler T P, Allen C K, Chan K C D et al. Experimental Study of Proton-beam Halo Induced by Beam Mismatch in LEDA. Proceedings of the 2001 PAC. Chicago, 2001. 2923–2925